Stroke Online Supplement

Table I. Checklist of Methodological and Reporting Aspects for Articles Submitted to *Stroke* Involving Preclinical Experimentation

Methodological and Reporting Aspects	Description of Procedures
Experimental groups and study timeline	☑ The experimental group(s) have been clearly defined in the article, including number of animals in each experimental arm of the study. ☑ An account of the control group is provided, and number of animals in the control group has been reported. If no controls were used, the rationale has been stated. ☑ An overall study timeline is provided.
Inclusion and exclusion criteria	☑ A priori inclusion and exclusion criteria for tested animals were defined and have been reported in the article.
Randomization	☑ Animals were randomly assigned to the experimental groups. If the work being submitted does not contain multiple experimental groups, or if random assignment was not used, adequate explanations have been provided. ☑ Type and methods of randomization have been described. ☑ Methods used for allocation concealment have been reported.
Blinding	☑ Blinding procedures have been described with regard to masking of group/treatment assignment from the experimenter. The rationale for nonblinding of the experimenter has been provided, if such was not feasible. ☑ Blinding procedures have been described with regard to masking of group assignment during outcome assessment.
Sample size and power calculations	☑ Formal sample size and power calculations were conducted based on a priori determined outcome(s) and treatment effect, and the data have been reported. A formal size assessment was not conducted and a rationale has been provided.
Data reporting and statistical methods	☑ Number of animals in each group: randomized, tested, lost to follow-up, or died have been reported. If the experimentation involves repeated measurements, the number of animals assessed at each time point is provided, for all experimental groups. ☑ Baseline data on assessed outcome(s) for all experimental groups have been reported. ☑ Details on important adverse events and death of animals during the course of experimentation have been provided, for all experimental arms. ☑ Statistical methods used have been reported. ☑ Numeric data on outcomes have been provided in text, or in a tabular format with the main article or as supplementary tables, in addition to the figures.
Experimental details, ethics, and funding statements	☑ Details on experimentation including stroke model, formulation and dosage of therapeutic agent, site and route of administration, use of anesthesia and analgesia, temperature control during experimentation, and postprocedural monitoring have been described. ☑ Different sex animals have been used. If not, the reason/justification is provided. ☑ Statements on approval by ethics boards and ethical conduct of studies have been provided. ☑ Statements on funding and conflicts of interests have been provided.

ONLINE SUPPLEMENT

RNA sequencing analysis revealed a distinct motor cortex transcriptome in spontaneously-recovered mice after stroke

Short Title: RNA-seq analysis of spontaneous recovery after stroke

Masaki Ito, MD, PhD; Markus Aswendt, PhD; Alex G. Lee, PhD; Shunsuke Ishizaka, MD, PhD; Zhijuan Cao, PhD; Eric H. Wang, BS; Sabrina L. Levy, BS; Daniel L. Smerin, BS; Jennifer A. McNab, PhD; Michael Zeineh, MD, PhD; Christoph Leuze, PhD; Maged Goubran, PhD; Michelle Y. Cheng, PhD; Gary K. Steinberg, MD, PhD

From the Department of Neurosurgery (M.I., M.A., S.I., Z.C., E.H.W., S.L.L., D.L.S., M.Y.C., G.K.S.), Department of Pediatrics (A.G.L.) and Department of Radiology (J.A.M., M.Z., C.L., M.G.), Stanford University School of Medicine, Stanford, CA,

M.I and M.A contributed equally to this work.
G.K.S and M.Y.C are co-senior authors.

Correspondence to Gary K. Steinberg, Stanford University Medical Center, 300 Pasteur Drive, R301A, MC 5325, Stanford, CA 94305, 650-725-5562, Email gsteinberg@stanford.edu, or Michelle Y. Cheng, Stanford University, Department of Neurosurgery, 1201 Welch Rd. MSLS P352, Stanford, CA 94305, 650-725-3111, Email mycheng@stanford.edu

Supplemental Methods

Animals

All mice were housed under a 12:12 hour light:dark cycle with food and water available *ad libitum*. As the goal of the study was to investigate a natural behavioral recovery after experimental stroke, we did not perform any treatment after stroke. A total of 75 mice were used in this study, of which 33 stroke mice and 7 non-stroke sham mice were included for analysis. Please see Figure I for the specific breakdown of the 75 mice we used in this study, with detailed inclusion/exclusion criteria. Sample size was calculated based on the performance of a pre- and post-stroke horizontal rotating beam test, mortality rate and presence of infarct after experimental stroke. Presence of cerebral infarct was evaluated by MRI (n = 22 mice) or histology (n = 11 mice) (see MRI and histology quantification sections in methods for details).

Transient middle cerebral artery occlusion

Mice were first anesthetized with 5% isoflurane and then maintained on 2–3% isoflurane. Compressed air flow was adjusted at 0.8L/min. The oxygen level in inhaled anesthetic gas was monitored (maxO2+, R217P72, Maxtec, West Valley City, UT, USA) and maintained at 40%–43%. Body temperature, heart rate, and respiration were monitored every 15 min and kept in physiological range. Artificial tears were used to prevent corneal damage. Under a surgical microscope, a midline ventral neck skin incision was made and an intraluminal 7-0 medium silicon rubber-coated filament (702045PK5Re; 0.20mm diameter and 4-5mm length with coating, Doccol Corporation, Sharon, MA, USA) was inserted from the left common carotid artery to the left middle cerebral artery (MCA) via internal carotid artery to block cerebral blood flow. The suture was left in place for 30 min and removed to allow reperfusion. Wounds were closed with suturing, and mice were administered an appropriate amount of 0.01mg/kg-body weight buprenorphine and 0.9% saline subcutaneously (s.c.). Mice were monitored for recovery and returned to their home cages. All mice were injected with 0.5ml of 0.9% saline s.c. every day for 7 days after stroke to prevent dehydration due to reduced mobility. Body weights for all mice were recorded before stroke and on PD 1, 4, 8 and 14. Mice were randomized, and the stroke surgeries were performed by an individual independent from behavior testing and analysis.

Behavior Tests

All behavior tests were performed by blinded observers on the day before stroke surgery and on PD 4, 8, and 14. Mice were handled and pre-trained every other day (three times) and the pre-stroke baseline data was collected the day before stroke. In the graphs, pre-stroke baseline is assigned to “day-1.”

Horizontal rotating beam test: This is a motor/sensory test that can detect neurological deficits in mice after transient MCAO, as descried in detail previously.[1,2] Briefly, the mouse was placed on a horizontal rotating beam (length 120 cm, diameter 13 mm, and 6 rotations per minute) and both the time and the distance traveled for each mouse were recorded. The rotating beam was situated at 60 cm above the floor, and the floor was covered with bubble cushions to reduce the impact from a fall. Three trials were performed for each mouse, of which the two highest values of distance (cm) and speed (cm/sec) were averaged for data analysis. The performance on this test was a central element in our inclusion and exclusion criteria (Please see Figure I in the online-only Data Supplement for inclusion/exclusion criteria).

Vertical stationary beam test was modified from Ogawa *et al*.:[3] Mice were placed with head downwards on top of a 51 cm long vertical pole (frosted fiber glass) with a diameter of 1.3 cm and allowed to descend the pole. The time it took the mouse to descend from the top of the beam to the floor was recorded. Three trials were performed per mouse. If the animal could not walk down but instead descended with a lateral body position or slip, then the result was recorded as "slip." If the mouse started to descend, but fell off the pole to the floor, the result was recorded as a "drop." The results were analyzed using a scoring system: a score of 4 was assigned when the mouse reached the floor within 6 seconds without a "slip" or "drop"; a score of 3 was assigned when the mouse reached the floor at 7 to 10 seconds without a "slip" or "drop"; a score of 2 was assigned when the mouse reached the floor at over 11 seconds without a "slip" or "drop"; score of 1 was assigned when the mouse slipped; and a score of 0 was assigned when the mouse dropped. From three trials the median of all scores was calculated for analysis.

Modified neurological score (mNS): We also assessed neurological function using the neurological scoring method described elsewhere,[4] with some modifications (Please see Table V in the online-only Data Supplement). Various aspects of neurological function were assessed, including general and focal deficits. In brief, general deficits were evaluated first by placing a mouse on an open bench top, and observing 5 categories of general deficits (hair, ears, eyes, spontaneous activity and epileptic behavior). A total score of 0 to 24 was assigned. Next, focal deficits were evaluated, composed of 6 categories (body symmetry, gait, circling behavior, forelimb symmetry, compulsory circling, whisker response), and a total score of 0 to 24 was assigned. Results were expressed as a composite neurological score of general and focal deficit categories, ranging from 0 (healthy) to 48 (the worst performance in all categories).

MRI & quantification of lesion volume

Mice were scanned at post-stroke day (PD) 2 with a 30cm horizontal bore 7-Tesla MRI system with 300mT/m gradients (GE/Bruker) using a 2-channel Millipede coil. Mice were kept anaesthetized during the scan with isoflurane (1.5-2% in air) and heated with warm air to keep the body temperature stable at 37°C. Qualitative T2-weighted images (T2WI) were acquired to cover the whole brain (Table I in the online-only Data Supplement) and used to quantify the individual infarct volume. Brain volumes were extracted using the BET algorithm of FSL (FMRIB Software Library; www.fmrib.ox.ac.uk/fsl). The hyperintensive area on T2WI was semi-automatically segmented into 3-dimension (3-D) using the snake evolution method of ITK-SNAP,[5] and the segmentation mask was applied onto the stroke lesion. The accuracy of the lesion mask was visually validated by independent observers (See Figure IIA for the representative images). For visualization, the 3-D surface of the brain extracted from T2WI and the 3-D surface of lesion segmentation mask was reconstructed with Amira (v3.1, FEI, Hillsboro, OR, USA). The ratio of the percentage of whole infarct voxels per whole brain voxels was calculated as % infarct volume, using MATLAB (v2007a, The MathWorks, Inc., Natick, MA, USA).

To evaluate lesion location, T2WI and the 25 μm Allen brain reference mouse atlas (ARA) were registered using a software pipeline [6] with tools from *ANTs* [7]. Briefly, an intensity-based b-spline, three-stage registration with increasing degrees of freedom of their transformations was applied: a) rigid, b) affine, and c) a non-rigid (deformable) b-spline symmetric normalization stage, each

consisting of a multi-resolution approach with 4 levels. Voxel-wise incidence maps of stroke lesion from both recovered and non-recovered mice were calculated by applying the registration to the 3-D stroke segmentation and counting the individual stroke voxel using MATLAB. Incidence maps are presented as % of mice with stroke lesion (Figure 2C). We selected 10 ARA labels for further analysis: somatosensory areas, somatomotor areas, striatum, temporal association areas, posterior parietal association areas, hippocampus regions, thalamus, basolateral amygdala nucleus, basomedial amygdala nucleus, and corticospinal tract, which are representative regions affected by transient MCA occlusion (MCAO). By applying the lesion masks to the labels (Figure IIA), the percentage of infarct voxels per total ARA label voxels was computed as % infarct volume per region, using MATLAB.

Immunofluorescence Staining

Mice were sacrificed on PD 15 and perfused transcardially with ice-cold phosphate buffered saline (PBS) followed by 3% paraformaldehyde (PFA). Brains were removed and cryo-protected overnight in a 20% sucrose/3% PFA solution. After brains sank to the bottom, they were frozen on dry ice and stored at -80°C until sectioning. Thirty-micrometer sections were cut using a cryostat and kept at -20°C in an antifreeze solution (30% ethylene glycol and 30% glycerol in PBS). Sections were first washed in PBS and then transferred to a blocking solution (10% normal animal serum, 1% bovine serum albumin in 0.3% PBS-triton X) for 1 hour, and incubated in a solution of primary antibody (1:500, CD68, ab53444, Abcam, Cambridge, UK) diluted in the blocking solution overnight at 4°C. The next day, sections were washed in 0.3% PBS-triton X and incubated with secondary antibody (1:500, Alexa Fluor 488, A11006, Invitrogen, Carlsbad, CA, USA) diluted in the blocking solution at room temperature for 2 hours. For staining with two primary antibodies, sections were processed with the following steps: first washed in PBS, next incubated with pre-heated 0.1M sodium citrate at 60°C for 20 minutes for antigen retrieval. After that, sections were transferred to a blocking solution (10% normal animal serum, 1% bovine serum albumin in 0.3% PBS-triton X) for 1 hour, and incubated in a solution of primary antibodies for CD68 (1:500, Abcam ab53444) and microtubule associated protein 2 (MAP2) (1:200, D5G1, Cell Signaling Technology, Danvers, MA, USA) diluted in the blocking solution overnight at 4 °C. The next day, sections were washed in 0.3% PBS-triton X and incubated with secondary antibodies (1:500, Alexa fluor 546, Invitrogen A11081 for CD68; and 1:500, Alexa fluor 488, Invitrogen A32731 for MAP2, respectively) diluted in the blocking solution at room temperature for 2 hours. DAPI (1:2000) was added during the last 5 minutes of the secondary antibody incubation. Sections were then washed in PBS, mounted, and cover-slipped.

Histology registration and lesion quantification

Infarct lesion area was identified by CD68-positive activated monocytes/macrophages. We confirmed that CD68-positive areas matched the MAP2-negative areas (neuronal loss). Images were captured using a CCD camera at 10x magnification (AxioCam MRm; Carl Zeiss AB, Switzerland), the Axio Imager M2 (Carl Zeiss AB, Switzerland), and the MBF software Neurolucida (MBF Bioscience, Williston, VT, USA). Stroke lesion quantification analyses were performed on coronal sections at the cortico-striatal (Str) level (range: 0.5 mm to 1.2 mm anterior to Bregma), and the thalamo-hippocampal (Hpx) level (range: 1.3 mm to 2.1 mm posterior to Bregma).

Lesion was verified using the automated method. Briefly, image slices were converted to NifTi format for image registration. For alignment of the original histology image and ARA, the corresponding ARA 25 um image was selected and scaled to the histology pixel dimensions manually. Landmark-based 2-D image registration was performed in 3-D Slicer (v4.6.2, http://www.slicer.org)[8] using the thin-plate spline algorithm. A set of 20–30 landmarks (fiducials) were placed on the moving (ARA) and fixed (histology) image to allow precise registration (Figure IIB). The resulting transformation was applied to the ARA template and labels. Registered images (ARA, ARA labels, microscopy channels) were combined as a stack in Image J (v1.5k, https://imagej.nih.gov/ij/). A manually defined lesion mask drawn on the CD68 images was used to automatically identify stroke-affected ARA regions for each mouse. Individual regions were summarized across all mice of both recovery groups and presented as % mice with infarct at striatal and hippocampal level, respectively (Figure 3C). The same 10 ARA region labels employed in the MRI analysis were utilized in the histology analysis. Similar to the analysis described in the MRI & quantification of lesion volume section, the percentage of whole infarct pixels per whole brain section pixels was calculated as % infarct area. We also computed % infarct area per region, which is the percentage of infarct area within the total area of each ARA region.

RNA Extraction

Eight stroke mice were selected and processed for RNA-seq analysis. These mice were also confirmed to show 1) similar pre-stroke baseline performance by horizontal rotating beam test, 2) similar stroke lesion evaluated by T2WI on post-stroke day 2, and 3) similar PD 4 deficits in horizontal rotating beam performance. At PD 15, mice were sacrificed and perfused with cold sterile PBS. Brains were removed and primary motor cortex, somatosensory cortex and striatum (from ipsi- and contralesional hemispheres) were dissected on ice with PBS and frozen in RNA later at −80°C. RNA from the brain samples were extracted using the Trizol reagent (Invitrogen) followed by QIAGEN RNeasy Plus kit (QIAGEN, Valencia, CA, USA). Briefly, each brain sample (~30mg) was homogenized for 1 minute in 1mL Trizol using the Qiagen Tissue Raptor. Chloroform (200ul) was added to the Trizol mixture and centrifuged for 15 min at 4°C. The top aqueous layer was transferred to a column for genomic DNA removal. RNA was precipitated with cold 70% ethanol and isolated using the company's instructions. Extracted RNA was stored at -80°C until further analysis. RNA quality was confirmed using the Agilent Bioanalyzer (Agilent, Santa Clara, CA, USA) and the RIN number for all samples ranged from 7 to 9. As a control group for quantitative PCR analysis, we selected 5 non-stroke sham mice and processed for RNA extraction as well.

RNA Sequencing and analysis

Eight stroke mice with comparable infarct in the striatum and somatosensory cortex were stringently selected from the 22 mice that were evaluated by MRI at PD 2. RNA samples from these 8 mice (total 16 samples: eight iM1 and eight cM1) were submitted to Stanford Functional Genomics Facility (Stanford University School of Medicine, Stanford, CA, USA) for cDNA library preparation and RNA sequencing. A cDNA library was prepared using the TruSeq Stranded mRNA Library Prep Kit. High-throughput sequencing of mature transcripts (RNA-seq) was performed using Hiseq 4000 (Illumina, Hayward, CA, USA) with read length of 2x75bp. The first lane was loaded with eight iM1 samples and the second lane was loaded with eight cM1 samples. After raw sequences were downloaded, quality check (QC) was performed using

FastQC, and sequence data was trimmed using Trimmomatic (version 0.36). STAR/2.5.1b (reference hg38.p5) was used for alignment and raw counts tabulation. R (version 3.1.1) was used for all downstream analysis. Briefly, counts were imported, and total mapped reads, unique to multiple map ratio and outliers were assessed for QC. Counts were normalized by trimmed mean of M-values (TMM) using the edgeR and scaled to library size. These counts were further precision weighted using the limma package with its voom method. DEGs were assessed separately (iM1 and cM1) using the limma package to run the linear model with empirical Bayes moderation. Overall, gene expression levels were reported as log2 CPM (counts per million). DEGs and expression fold change were represented by comparison between "recovered"/"non-recovered" in either the iM1 or cM1 (imposed minimum threshold: $P<0.05$). The DEGs in iM1 and cM1 were further analyzed by Ingenuity Pathway Analysis (IPA) software (QIAGEN) in order to provide the significant canonical pathway, diseases and functions of the DEGs in iM1 and cM1 (Imposed minimum threshold: $P<0.05$, absolute expression log fold change>0.26). P-values and ratios for these pathways were plotted. P-values for the significance of each pathway were computed based on those number of genes involved in the pathway by using Fisher's exact test, and negatively log10 transformed. Ratio expresses the number of DEGs in our dataset over total number of genes in each canonical pathway based on the IPA knowledge database. IPA software provided a pathway activity Z-score for eligible canonical pathways based on expression fold change data of one or more molecules in each pathway. A positive Z-score indicates that the pathway is predicted to be activated, and a negative Z-score predicts inhibition. For correlation analysis, Spearman correlation was used to compare behavioral recovery (distance at PD 14) with each DEG (Imposed minimum threshold: $P<0.05$, absolute expression log fold change>0.26).

Quantitative PCR

To further validate the results from the RNA-seq analysis, we performed quantitative real-time PCR (qPCR) for selected genes of interest in various brain regions including M1, somatosensory cortices (S), and striatum (Str) from the contralesional hemisphere of stroke mice and non-stroke sham mice. First-strand cDNA synthesis was performed using the High-Capacity cDNA Reverse Transcription Kit (4368814, Applied Biosystems, Foster city, CA, USA). qPCR was performed using the CFX96 Real-Time PCR Detection system (Bio-Rad Laboratories Inc., Hercules, CA, USA). qPCR reaction mixtures were prepared using the Taqman gene expression master mix (4369016, Applied Biosystems) and Taqman gene expression assays (Thermo Fisher Scientific, Waltham, MA, USA) targeting mouse Adora2a (Mm00802075_m1), Drd2 (Mm00438545_m1), Pde10a (Mm00449329_m1), and GAPDH (Mm99999915_g1). GAPDH was used as the housekeeping gene. qPCR data were analyzed using the Delta Delta CT method with Pfaffl correction for efficiency [9].

References

1. Cheng MY, Wang EH, Woodson WJ, Wang S, Sun G, Lee AG, et al. Optogenetic neuronal stimulation promotes functional recovery after stroke. *Proc. Natl. Acad. Sci.* 2014;111:12913–12918.
2. Shah AM, Ishizaka S, Cheng MY, Wang EH, Bautista AR, Levy S, et al. Optogenetic neuronal stimulation of the lateral cerebellar nucleus promotes persistent functional

recovery after stroke. *Sci. Rep.* 2017;7:46612.
3. Ogawa N, Hirose Y, Ohara S, Ono T, Watanabe Y. A simple quantitative bradykinesia test in MPTP-treated mice. *Res Commun Chem Pathol Pharmacol*. 1985;50:435–441.
4. Garcia JH, Wagner S, Liu KF, Hu XJ. Neurological deficit and extent of neuronal necrosis attributable to middle cerebral artery occlusion in rats. Statistical validation. *Stroke*. 1995;26:627–34; discussion 635.
5. Yushkevich PA, Piven J, Hazlett HC, Smith RG, Ho S, Gee JC, et al. User-guided 3D active contour segmentation of anatomical structures: Significantly improved efficiency and reliability. *Neuroimage*. 2006;31:1116–1128.
6. Goubran M. [Abstract] Multimodal image registration and analysis via clarity-based light-microscopy (MIRACL). Society for Neurocience, 92.10 / KKK8 (2016). Available from: http://www.abstractsonline.com/pp8/#!/4071/presentation/14593
7. Avants BB, Tustison NJ, Song G, Cook PA, Klein A, Gee JC. A reproducible evaluation of ANTs similarity metric performance in brain image registration. *Neuroimage*. 2011;54:2033–2044.
8. Fedorov A, Beichel R, Kalpathy-Cramer J, Finet J, Fillion-Robin JC, Pujol S, et al. 3D Slicer as an image computing platform for the Quantitative Imaging Network. *Magn. Reson. Imaging*. 2012;30:1323–1341.
9. Pfaffl MW. A new mathematical model for relative quantification in real-time RT-PCR. *Nucleic Acids Res.* 2001;29:e45.

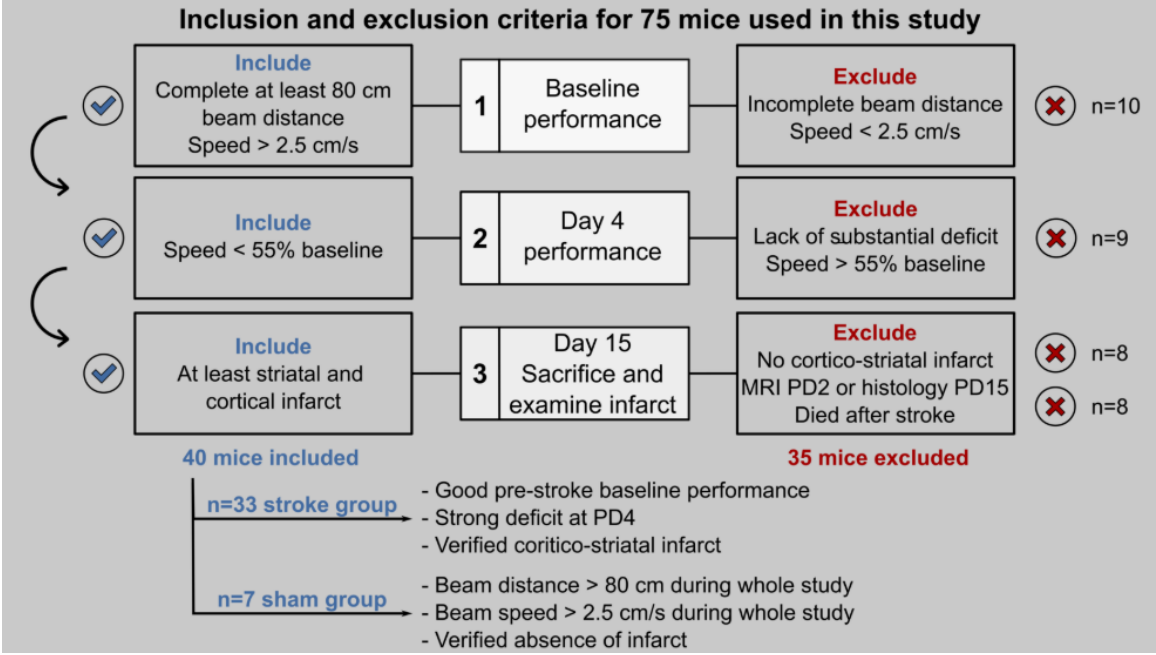

Figure I: The breakdown of detailed inclusion/exclusion criteria

Diagram showing the specific breakdown of the 75 mice used in this study, with detailed descriptions for the inclusion/exclusion criteria.

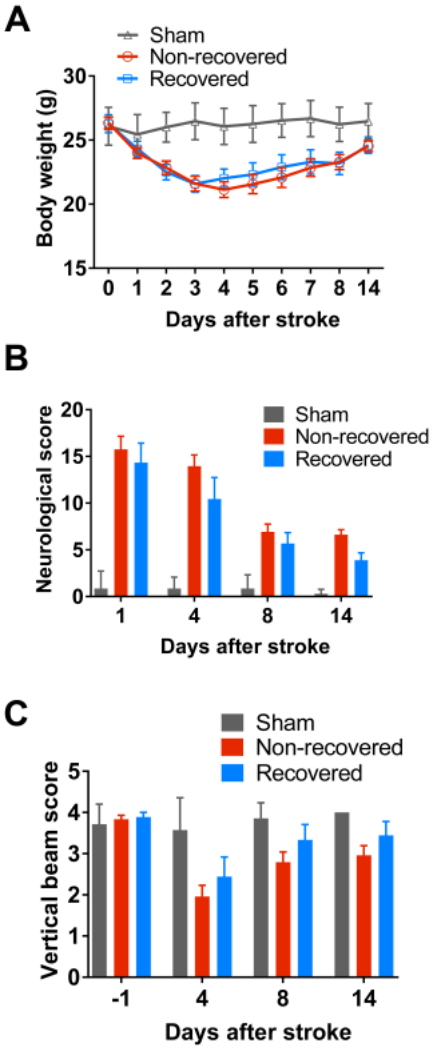

Figure II. Overview of change in body weight (*A*), neurological score (*B*) and vertical beam score (*C*).

A, Line graphs (mean±SEM) showed chronological change of mean body weight in recovered and non-recovered mice (n = 9 and 24 mice, respectively) and non-stroke sham mice (n = 7). **B,** Bar graphs with error bars (mean±SEM) showed chronological change of modified neurological score in recovered and non-recovered mice (n = 9 and 24 mice, respectively) and non-stroke sham mice (n = 7). **C,** Bar graphs with error bars (mean±SEM) showed chronological change of vertical beam score in recovered and non-recovered mice (n = 9 and 24 mice, respectively) and non-stroke sham mice (n = 7).

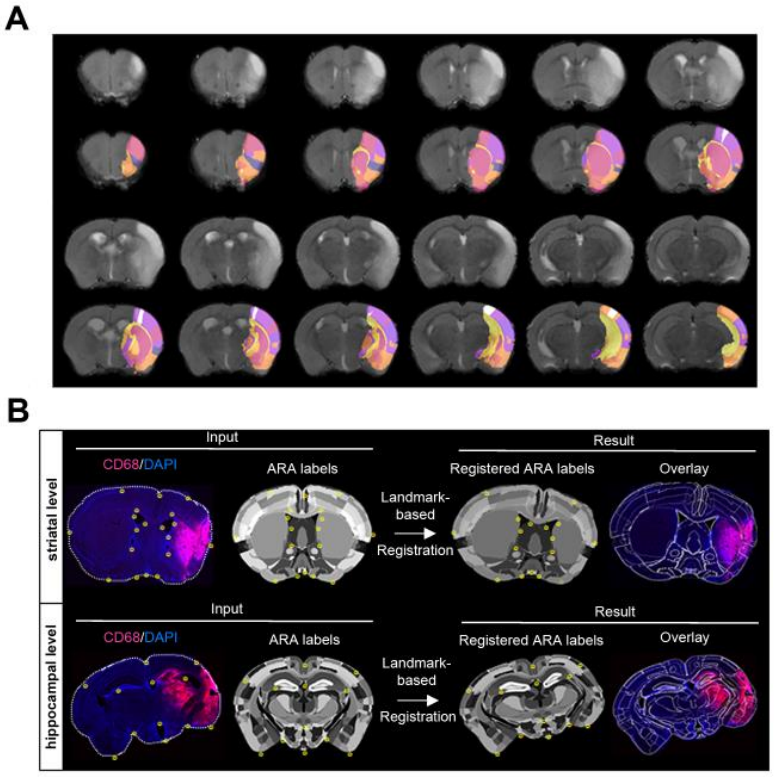

Figure III. Verification of co-registrations for MRI/histology and Allen brain mouse atlas. **A,** Representative legion masks of cerebral infarct semi-automatically registered on corresponding hyperintensive area on T2WI were depicted at consecutive coronal brain slices. Note that each lesion mask was segmented per brain region based on the Allen brain reference mouse atlas (ARA) labels. **B,** Workflow of landmark-based registration in Slicer3D was shown for two representative CD68/DAPI microscopy images at striatal and hippocampal levels. Manually set landmarks (yellow circles) on both images and the ARA labels were matched by the algorithm, which was used to warp the labels onto the image.

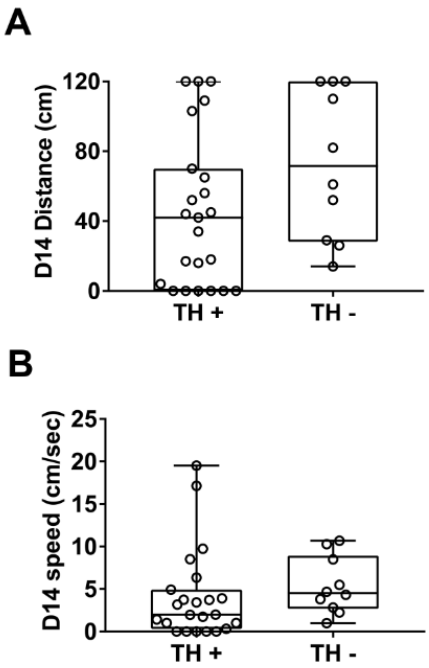

Figure IV. Correlation analysis of rotating beam results and infarct in the thalamus. Box and whisker plots with individual plots demonstrated the results of horizontal rotating beam performance at post-stroke (PD) day 14 (distance **A** and speed **B**) in mice with or without the thalamus (TH) lesion (n = 23 and 10 mice, respectively) based on the lesion evaluation by MRI (PD 2 for 22 mice) or histology (PD 15 for 11 mice). Whiskers express maximum and minimal values of beam performance. No significant correlation was detected between TH lesion and recovery (PD 14) (distance: Spearman r = -0.101, *P*=0.781; speed: Spearman r = 0.178, *P*=0.63).

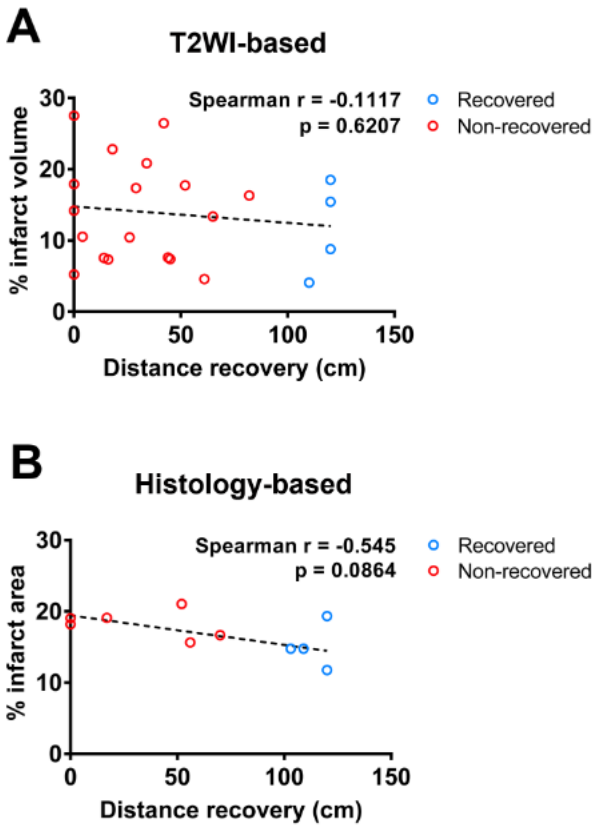

Figure V. Correlation analysis of rotating beam results and infarct size. Scatter plots demonstrated no significant correlations (Spearman) between the behavior recovery outcome (rotating beam distance at post-stroke day (PD) 14) and % infarct volume evaluated by T2WI at PD2 (n=4 recovered, n=18 non-recovered mice) or % infarct area evaluated by CD68 immunostaining at PD15 (n=5 recovered, n=6 non-recovered mice). Each line depicted linear regression for each scatter plot. % infarct area at the cortico-striatal and thalamo-hippocampal coronal section level were averaged in each individual mouse. No significant correlation was detected between infarct size (% infarct volume by T2WI or % infarct area by histology) and recovery (PD 14) (% infarct volume: Spearman r = -0.01, $P = 0.621$; % infarct area: Spearman r = -0.545, $P = 0.086$).

Table I. Parameters for T2WI.

MRI machine	Repetition Time (ms)	Effective Echo Time (ms)	Matrix	Field of View (cm)	Resolution (um)	Scan Time
GE	5200	40	256x256x64	3.00x3.00x1.00	117x117x1000	7 min 30 sec
Bruker	4500	45	256x256x64	2.56x2.56x0.5	100x100x500	

Table II. Gene symbols and their names used in the main manuscript body

Gene Symbol	Entrez Gene Name
Adora2a	Adenosine A2a receptor
Alx4	Aristaless-like homeobox 4
Aox3	Aldehyde oxidase 3
C3	Complement component 3
Cdca7	Cell division cycle associated 7
Col15a1	Collagen type XV alpha 1 chain
Dcaf12l2	DDB1 and CUL4 associated factor 12-like 2
Drd2	Dopamine receptor D2
GAPDH	Glyceraldehyde-3-phosphate dehydrogenase
Gpnmb	Transmembrane glycoprotein nmb
Hbb.bs	Hemoglobin, beta adult s chain
Hbb.bt	Hemoglobin, beta adult t chain
Lrrc10b	Leucine rich repeat containing 10B
Lyve1	Lymphatic vessel endothelial hyaluronan receptor 1
Neat1	Nuclear paraspeckle assembly transcript 1
Npas 4	Neuronal PAS domain protein 4
Pde10a	Phosphodiesterase 10A
Ptger4	Prostaglandin E receptor 4
Skap1	Src kinase associated phosphoprotein 1
Tfap2b	Transcription factor AP-2 beta
Tnfaip2	Tumor necrosis factor, alpha-induced protein 2
Trhr	Thyrotropin releasing hormone receptor

Table III. A panel of recovery-related differentially expressed genes in the iM1
A list of differentially expressed genes (DEGs) in the iM1 of spontaneously-recovered mice with significant correlation to the recovery outcome (38 genes)

Gene Symbol	Entrez Gene Name	RNA-seq Gene Expression Analysis		Correlation Analysis with Recovery	
		Log FC	*P* value	Spearman R	*P* value
Ankrd6	ankyrin repeat domain 6	-0.375	<0.0001	-0.898	0.002
Arhgap6	Rho GTPase activating protein 6	-0.549	0.009	-0.874	0.005
Bach2	BTB domain and CNC homolog 2	-0.31	0.05	-0.731	0.04
Btaf1	B-TFIID TATA-box binding protein associated factor 1	0.359	0.003	0.874	0.005
Casp1	caspase 1	0.458	0.046	0.79	0.02
Cited4	Cbp/p300 interacting transactivator with Glu/Asp rich	-0.307	0.046	-0.826	0.011
Ctnna3	catenin alpha 3	-0.486	0.037	-0.79	0.02
Dcdc2a	doublecortin domain containing 2	0.275	0.047	0.826	0.011
Eme2	essential meiotic structure-specific endonuclease subunit 2	-0.308	0.036	-0.731	0.04
Epha8	EPH receptor A8	-0.392	0.031	-0.802	0.017
Fdx1	ferredoxin 1	-0.347	0.017	-0.826	0.011
Gpr137b	G protein-coupled receptor 137B	0.276	0.032	0.731	0.04
Hpse	heparanase	0.904	0.009	0.898	0.002
Hrk	harakiri, BCL2 interacting protein (contains only BH3	-0.33	0.017	-0.731	0.04
Ide	insulin degrading enzyme	0.408	0.001	0.755	0.031
Kcns3	potassium voltage-gated channel modifier subfamily S	0.289	0.032	0.862	0.006
Krt73	keratin 73	-0.744	0.013	-0.802	0.017
Lrrc10b	leucine rich repeat containing 10B	-0.646	0.021	-0.826	0.011
Mapk12	mitogen-activated protein kinase 12	-0.566	0.007	-0.755	0.031
Mybpc1	myosin binding protein C, slow type	0.429	0.006	0.826	0.011
Ndst3	N-deacetylase and N-sulfotransferase 3	-0.379	<0.0001	-0.778	0.023
Nefh	neurofilament heavy	0.306	<0.0001	0.755	0.031
Nefm	neurofilament, medium polypeptide	0.261	0.019	0.743	0.035
Neurl1a	neuralized E3 ubiquitin protein ligase 1	-0.264	0.001	-0.731	0.04
Nhs	NHS actin remodeling regulator	0.32	0.037	0.766	0.027
Nrtn	neurturin	-0.556	0.016	-0.946	<0.0001
Pcdha12	protocadherin alpha 13	0.353	0.016	0.934	0.001
Pde10a	phosphodiesterase 10A	-0.317	0.015	-0.731	0.04
Pde11a	phosphodiesterase 11A	-0.414	0.028	-0.826	0.011
Pidd1	p53-induced death domain protein 1	0.783	0.003	0.802	0.017
Sag	S-antigen visual arrestin	-0.482	0.027	-0.826	0.011
Scn1a	sodium voltage-gated channel alpha subunit 1	0.275	0.007	0.743	0.035
Syt2	synaptotagmin 2	0.359	0.006	0.743	0.035
Tmem81	transmembrane protein 81	0.365	0.048	0.874	0.005
Tpbg	trophoblast glycoprotein	0.358	0.012	0.731	0.04
Unc5b	unc-5 netrin receptor B	0.351	0.016	0.755	0.031
Xkr7	XK related 7	0.38	0.044	0.79	0.02
Zpbp	zona pellucida binding protein	0.66	0.011	0.886	0.003

Table IV. A panel of recovery-related differentially expressed genes in the cM1
A list of differentially expressed genes (DEGs) in the cM1 of spontaneously-recovered mice with significant correlation to the recovery outcome (74 genes)

Gene Symbol	Entrez Gene Name	RNA-seq Gene Expression Analysis		Correlation Analysis with Recovery	
		Log FC	*P* value	Spearman R	*P* value
Adora2a	adenosine A2a receptor	-0.861	0.007	-0.743	0.035
Aim2	absent in melanoma 2	-0.496	0.043	-0.826	0.011
Apool	apolipoprotein O like	0.336	0.047	0.731	0.04
Arhgef37	Rho guanine nucleotide exchange factor 37	-0.466	0.033	-0.838	0.009
Atg4a	autophagy related 4A cysteine peptidase	-0.321	0.048	-0.922	0.001
Bach2	BTB domain and CNC homolog 2	-0.397	0.003	-0.922	0.001
BC028528	chromosome 1 open reading frame 54	-0.466	0.025	-0.934	0.001
Bub1b	BUB1 mitotic checkpoint serine/threonine kinase B	-0.844	0.008	-0.814	0.014
Cd83	CD83 molecule	0.267	0.018	0.85	0.007
Cdca7	cell division cycle associated 7	-0.862	0.002	-0.898	0.002
Cenpl	centromere protein L	-0.565	0.018	-0.958	<0.0001
Ciart	circadian associated repressor of transcription	-0.274	0.046	-0.766	0.027
Cntnap5b	contactin associated protein-like 5B	-0.414	<0.0001	-0.731	0.04
Commd1	copper metabolism domain containing 1	0.28	0.021	0.922	0.001
Cox16	COX16, cytochrome c oxidase assembly homolog	-0.566	0.02	-0.79	0.02
Dcaf12l2	DDB1 and CUL4 associated factor 12 like 2	0.577	0.022	0.778	0.023
Disp1	dispatched RND transporter family member 1	0.29	0.028	0.79	0.02
Dnah1	dynein axonemal heavy chain 1	-0.272	0.041	-0.731	0.04
Drd2	dopamine receptor D2	-1.597	<0.0001	-0.91	0.002
Eya4	EYA transcriptional coactivator and phosphatase 4	-0.282	0.012	-0.743	0.035
Fgfbp3	fibroblast growth factor binding protein 3	0.287	0.028	0.898	0.002
Flnb	filamin B	-0.295	0.001	-0.802	0.017
Glcci1	glucocorticoid induced 1	-0.431	0.006	-0.755	0.031
Gpr6	G protein-coupled receptor 6	-0.791	0.003	-0.958	<0.0001
Gpr68	G protein-coupled receptor 68	0.319	0.01	0.766	0.027
Hmmr	hyaluronan mediated motility receptor	-0.542	0.017	-0.731	0.04
Islr	immunoglobulin superfamily containing leucine rich repeat	-0.304	0.043	-0.778	0.023
Itpkc	inositol-trisphosphate 3-kinase C	0.27	0.027	0.731	0.04
Kcne4	potassium voltage-gated channel subfamily E regulatory subunit 4	-0.653	0.013	-0.814	0.014
Kctd11	potassium channel tetramerization domain containing 11	-0.499	0.022	-0.719	0.045
Lct	lactase	-0.508	0.028	-0.826	0.011
Lekr1	leucine, glutamate and lysine rich 1	-0.372	0.041	-0.826	0.011
Lrrc10b	leucine rich repeat containing 10B	-0.885	0.009	-0.79	0.02
Mas1	MAS1 proto-oncogene, G protein-coupled receptor	0.264	0.006	0.778	0.023
Micall2	MICAL like 2	0.433	0.029	0.862	0.006
Mme	membrane metalloendopeptidase	-0.266	0.031	-0.79	0.02
Myl9	myosin light chain 9	-0.348	0.006	-0.731	0.04
Myt1	myelin transcription factor 1	-0.369	0.009	-0.826	0.011
Naaladl2	N-acetylated alpha-linked acidic dipeptidase like 2	-0.527	<0.0001	-0.826	0.011
Nek8	NIMA related kinase 8	0.491	0.016	0.79	0.02
Nemp2	nuclear envelope integral membrane protein 2	-0.352	0.032	-0.874	0.005
Ninl	ninein like	0.298	0.017	0.97	<0.0001
Npl	N-acetylneuraminate pyruvate lyase	-0.412	0.015	-0.719	0.045
P2ry1	purinergic receptor P2Y1	-0.551	0.005	-0.826	0.011
Paox	polyamine oxidase	0.413	0.01	0.731	0.04
Pcdhb6	protocadherin beta 6	-0.454	0.008	-0.719	0.045
Pcdhb9	protocadherin beta 9	0.366	0.001	0.898	0.002
Pde10a	phosphodiesterase 10A	-0.51	<0.0001	-0.946	<0.0001

Gene Symbol	Entrez Gene Name	RNA-seq Gene Expression Analysis		Correlation Analysis with Recovery	
		Log FC	*P* value	Spearman R	*P* value
Plce1	phospholipase C epsilon 1	-0.312	0.01	-0.755	0.031
Plk4	polo like kinase 4	-0.305	0.048	-0.743	0.035
Plp2	proteolipid protein 2	0.347	0.04	0.755	0.031
Polr1e	RNA polymerase I subunit E	-0.309	0.018	-0.778	0.023
Prss22	protease, serine 22	0.491	0.019	0.755	0.031
Pstpip2	proline-serine-threonine phosphatase interacting protein 2	-0.335	0.044	-0.898	0.002
Ptger4	prostaglandin E receptor 4	-0.625	0.008	-0.838	0.009
Qtrtd1	Queuine TRNA-Ribosyltransferase Domain Containing 1	-0.272	0.015	-0.862	0.006
Rab27a	RAB27A, member RAS oncogene family	-0.306	0.034	-0.862	0.006
Rbm4	RNA binding motif protein 4	-0.393	0.03	-0.874	0.005
Rxrg	retinoid X receptor gamma	-0.656	0.021	-0.755	0.031
Slc25a24	solute carrier family 25 member 24	-0.424	0.007	-0.731	0.04
Slc25a30	solute carrier family 25 member 30	-0.294	0.046	-0.766	0.027
Slc44a5	solute carrier family 44 member 5	0.302	0.02	0.731	0.04
Sorcs3	sortilin related VPS10 domain containing receptor 3	0.297	0.004	0.886	0.003
Sox11	SRY-box 11	-0.334	0.004	-0.766	0.027
Spag4	sperm associated antigen 4	-0.38	0.05	-0.743	0.035
Supt3	SPT3 homolog, SAGA and STAGA complex component	0.271	0.012	0.719	0.045
Syndig1l	synapse differentiation inducing 1 like	-0.769	0.034	-0.755	0.031
Tmem181b.ps	transmembrane protein 181B, pseudogene	-0.542	<0.0001	-0.874	0.005
Trmt13	tRNA methyltransferase 13 homolog	-0.448	0.015	-0.826	0.011
Trp53inp1	tumor protein p53 inducible nuclear protein 1	-0.283	0.004	-0.85	0.007
Vav1	vav guanine nucleotide exchange factor 1	0.348	0.034	0.743	0.035
Zfp280c	zinc finger protein 280C	-0.349	0.004	-0.79	0.02
Zfp566	zinc finger protein 566	-0.447	0.019	-0.85	0.007
Zscan29	zinc finger and SCAN domain containing 29	-0.369	0.003	-0.922	0.001

Table V. Categories and scores for general and focal deficits evaluated in modified neurological scoring in this study

General deficits (total score 0 to 24)

1. Hair (score 0 - 2)
score 0: hair neat and clean
score 1: localized piloerection and dirty hair in 2 body parts
score 2: piloerection and dirty hair in more than 2 body parts
2. Ears (score 0 - 2)
score 0: ears are stretched laterally and behind with reaction to noise
score 1: one or both of ears are stretched laterally but not behind with reaction to noise
score 2: same as 1 but they do not react to noise
3. Eyes (score 0 - 4)
score 0: open, clean and quickly follow the surrounding environment
score 1: open and characterized by aqueous mucus. Slowly follow the surrounding environment
score 2: open and characterized by dark mucus
score 3: ellipsoidal shaped and characterized by dark mucus
score 4: closed
4. Spontaneous activity (score 0 - 4)
score 0: alert and explores actively
score 1: seems alert, but calm and sluggish
score 2: mouse explores intermittently and sluggishly
score 3: somnolent and numb, few movements on-the-spot
score 4: no spontaneous movements
5. Epileptic behavior (score 0 - 12), The worse epileptic behavior detected during the whole observational period should be recorded and reported according to the following score.
score 0: none
score 3: mouse is reluctant to handling, shows hyperactivity
score 6: mouse is aggressive, stressed and stares
score 9: mouse shows hyper-excitability, chaotic movements and presence of convulsion following handling
score 12: generalized seizures associated with wheezing and un-consciousness

Focal deficits (total score 0 to 24)

6. Body symmetry (score 0 - 4), Mouse on open bench top and observation of undisturbed resting behavior and description of the virtual nose-tail line
score 0: normal, body in normal posture, trunk elevated from bench, with fore- and hind-limbs leaning beneath the body. Tail straight
score 1: slight asymmetry, body leans on one side with fore- and hind-limbs leaning beneath the body, tail slightly bent
score 2: moderate asymmetry, body leans on one side with fore- and hind-limbs stretched out, tail slightly bent
score 3: prominent asymmetry, body bent, on one side lies on the bench, tail bent
score 4: extreme asymmetry, body highly bent on one side constantly lies on the bench, tail highly bent
7. Gait (Score 0 - 4), Mouse on open top bench, observation of undisturbed movements
score 0: normal, gait is flexible, symmetric and quick
score 1: stiff, inflexible. mouse walks humpbacked slower than normal mice
score 2: limping with asymmetric movements
score 3: trembling, drifting, falling
score4: does not walk spontaneously. In this case, stimulation will be performed gently pushing the mouse with a pen. When stimulated, the mouse walks no longer than 3 steps)
8. Circling behavior (score 0 - 4), observation of the mouse walking undisturbed on the open top bench score 0: absent. mouse equally turns left or right
score 1: predominantly one-sided turns
score 2: circles to one side, although not constantly
score 3: circles constantly to one side
score 4: pivoting, swaying, or no movement
9. Forelimb symmetry (score 0 - 4), Mouse suspended by the tail. Movements and position of forelimbs are observed.
score 0: normal. Both forelimbs are extended towards the bench and move actively
score 1: light asymmetry, contralateral forelimb does not extend entirely
score 2: marked asymmetry, contralateral forelimb bends towards the trunk. the body slightly bends on the ipsilateral side
score 3: prominent asymmetry, contralateral forelimb adheres to the trunk
score 4: slight asymmetry, no body/limb movement
10. Compulsory circling (score 0 - 4), forelimbs on the bench, hind-limbs suspended by the tail. This position reveals the presence of the contralateral limb palsy.
score 0: absent. normal extension of both forelimbs
score 1: tendency to turn to one side, the mouse extends both forelimbs, but starts to turn preferably to one side

score 2: circles to one side. the mouse turns towards one side with a slower movement compared to healthy side
score 3: pivots to one side sluggishly. the mouse turns towards one side failing to perform a complete circle
score 4: does not advance. the front part of the trunk lies on the bench. slow and brief movements
11. Whisker response (score 0 - 4), mouse on the bench. using a pen, touch gently the whiskers and the tip of ears from behind, first one the lesioned and then on the contralateral side
score 0: normal symmetrical response. Mouse turns the head towards the stimulated side and withdraws from the stimulus
score 1: light asymmetry, the mouse withdraws slowly when stimulated on the ischemic side, normal response on the contralateral side
score 2: prominent asymmetry, no response when stimulated on the ischemic side, normal response on the contralateral side
score 3: absent response ipsilaterally, slow response when stimulated on the contralateral side
score 4: absent response bilaterally